CELLULOSE CHEMISTRY AND TECHNOLOGY

APPLICATION OF EXPERIMENTAL DESIGN FOR OPTIMIZATION OF MALACHITE GREEN REMOVAL BY TETRAETHYLENEPENTAMINE MODIFIED PEANUT HUSK COMPOSITE BEADS

KAH-TONG CHAN,[*] SIEW-TENG ONG[*,**] and SIE-TIONG HA[*,**]

[*]*Faculty of Science, Universiti Tunku Abdul Rahman, 31900 Kampar, Perak, Malaysia*
[**]*Centre for Agriculture and Food Research, Universiti Tunku Abdul Rahman,*
31900 Kampar, Perak, Malaysia
✉ *Corresponding author: S.-T. Ong, ongst@utar.edu.my, ongst_utar@yahoo.com*

Received September 5, 2024

Batch and experimental design experiments were performed in this study to assess the effectiveness of chemically modified peanut husks (tepaPH) beads as a sorbent for Malachite Green (MG). For the identification of the functional groups on tepaPH (before and after adsorption), IR spectrum analysis was performed. Surface analyses were performed by using atomic force microscope and scanning electron microscopy. The effectiveness of tepaPH in the removal of MG was studied under different experimental conditions, varying the agitation rate, initial MG concentration, contact time, pH, and contact time. The experimental results revealed that the kinetics of the MG adsorption process can be reasonably explained by the pseudo-2nd-order kinetic model. From the linearized Langmuir isotherm equation, the maximum adsorption capacity for MG by tepaPH beads was calculated to be 9.6339 mg/g. The isotherm data were fitted into various isotherm models' equations and the Freundlich isotherm model appeared to provide reasonable fitting with high R^2 values. The adsorption model was optimized by using statistical tools, such as Plackett-Burman design and response surface methodology. Under the optimum conditions (0.6 g of tepaPH, 50 mg/L of MG dye concentration and 480 minutes contact time), a high percentage uptake of MG, of 93.98%, was achievable.

***Keywords**:* Malachite Green, tetraethylenepentamine, Plackett-Burman design, response surface methodology, peanut husk

INTRODUCTION

One of the biggest concerns in the control of environmental pollution is water pollution. Water is a vital resource for every living organism and clear water is crucial for maintaining ecosystem balance. However, due to the high usage of dyes and pigments in paper, plastic, and textile industries,[1] water contamination caused by these industries has become a major concern. Each year, more than 15% of the total production of dyes is being disposed of, without proper treatment, from industrial wastewater streams into rivers, oceans and lakes.[2,3] Thus, the ecosystems are seriously affected. Some of the conventional methods for pollutant removal from the effluents include adsorption, electrochemical treatments, anaerobic and aerobic microbial degradation, ion exchange, reverse osmosis, chemical oxidation, filtration, coagulation, and chemical precipitation.[2,4,5]

The adsorption technique has a widespread application due to its high efficiency, simple design of experiment and easy operation.[2,5,6] It is a separation process that will not form any harmful intermediates or toxic end products and will not alter the structure and characteristics of the pollutants.[7–11] The adsorbates are accumulated on the adsorbent's surface and may be recovered through desorption processes.[6,9] The adsorption of pollutants by low-cost agricultural waste is considered as an economical approach, as such adsorbents have high removal efficiency and can be regenerated easily.[10,12–15]

Malachite Green (MG) is a synthetic cationic triarylmethane dye containing the triphenylmethane backbone. It is a water soluble dye that dissociates in aqueous solution to form positively charged ions.[6,16,17] It is widely used for dyeing products such as leather, paper, silk, cotton,

Cellulose Chem. Technol., ***59*** *(1-2), 207-221(2025)*

wool and other textiles.[3,18–20] In aquafarming, it is often used as pesticide, bactericide, and fungicide. Besides, it is also being utilized in different fields, for instance, medical and food industry.[6,11,16,21] Although MG has a widespread application in different industries, it is highly toxic, mutagenic, teratogenic, and carcinogenic. All these may lead to a negative impact on human health, causing chromosomal fractures, cancer, eye irritation, and organs' damage.[16,17,19,22] For that reason, several studies have reported using different adsorbents for the removal of MG, such as magnetic amino-modified lignin,[23] waste crab shells,[24] *Elaeagnus angustifolia* seeds activated carbon,[25] *Cycas* leaves powder,[6] rambutan peel-based activated carbon[26] and NaOH modified pine cone.[17] The total worldwide production of peanut was 51.32 million metric tons in year 2024. China has contributed 19 million metric tons of production, which makes it the country with the highest peanut production.[27] The peanut kernels are consumed, but the peanut husks are usually discarded and considered as agro-waste. Thirty percent of the weight of peanut are from the husks. However, peanut husks can be utilized as an adsorbent to eliminate pollutants from wastewater. Phenolic acid, hydroxyl, and carboxylic groups can be found on the surface of peanut husks, as they are mainly composed of lignin, hemicelluloses, and cellulose.[28,29]

The current work aimed to determine the effectiveness of chemically modified peanut husk beads (tepaPH beads) in the removal of MG. The adsorption experimental results were studied using different kinetic and isotherm models.

The effect of various parameters was studied in batch studies. Besides, the relationship between each parameter in affecting the MG uptake was investigated, using the Plackett-Burman design (PB) and response surface methodology (RSM), the latter being used to obtain the optimum conditions for MG dye uptake.

EXPERIMENTAL

Chemicals

Malachite Green (MG, C.I. = 40000), tetraethylenepentamine (TEPA, technical grade) and sodium alginate were purchased from Sigma-Aldrich. Calcium chloride (anhydrous powder) was purchased from Merck and used as a crosslinking agent. No further purification step was carried out and the chemicals were all used as received.

Preparation of tepaPH powder

Peanut husk (PH) was obtained by shelling peanuts purchased from a local store in Malaysia. The collected peanut husks were washed several times with water to ensure the removal of ash and any adhering particles. After being dried completely, a grinder was used to turn the PH to a more homogenous particle size. The PH was screened through a set of sieves, and the PH particle size fraction from 250 to 425 μm was used in this study. Chemically modified PH was obtained by treating one gram of PH with 0.02 mol of TEPA. This mixture was then subjected to heating at 90 °C by using water bath for three hours under intermittent stirring. The modified product was washed with distilled water until neutral and labelled as tepaPH powder.

Preparation of tepaPH beads

For the formation of tepaPH beads, a homogenous mixture of 6 mL of 3% sodium alginate solution and 1.00 g of tepaPH powder were added into a 4% calcium chloride ($CaCl_2$) bath dropwise. The residual $CaCl_2$ was removed from the beads by washing them with distilled water. The reaction product was then subjected to drying at 60 °C in the oven. Finally, the obtained beads were labelled as tepaPH beads.

Characterization study

The surface functional groups of the adsorbents before and after adsorption were determined using a Perkin Elmer ATR-FTIR, model Spectrum Two FT-IR Spectrometer, in the scanning range from 4000 to 400 cm^{-1}. A Scanning Electron Microscope (SEM) model JEOL-JSM-6701F was used to study the adsorbents' surface morphology. The adsorbent's surface was studied at 10000× magnification using 4.0 kV emissions current. A Park Systems Atomic Force Microscope (AFM), model XE-70, was used to detect changes in surface structure on the atomic scale. The scan rate and scan size were fixed at 0.8 Hz and 1.5 × 1.5 μm, respectively.

Batch studies

All the batch experiments were carried out in duplicates and the mean results were presented. The adsorption experiments were performed by pouring 20 mL of MG dye solution into a centrifuge tube with 0.20 g of tepaPH beads. The mixtures were then subjected to agitation on an orbital shaker at 150 rpm. To make sure that the centrifuge tube wall does not contribute to the uptake of dye, a control test (without tepaPH beads) was carried out concurrently. The supernatant's absorbance was determined using a double beam UV-Vis spectrophotometer for the calculation of dye concentration. The influence of various operating parameters on the adsorption efficiency was included in this work.

Optimization studies

PB and RSM were performed using the Design Expert Version 7.1.3. In PB, the adsorbent dosage, initial MG concentrations, agitation rates, and contact time were the chosen factors to be examined. The significant factors identified through PB were then incorporated into RSM for further investigation to identify the optimum conditions that allow obtaining the highest uptake of MG. All the experiments were conducted in duplicates and the mean values of the duplicates were taken as the response (percentage uptake of MG).

Regeneration and reusability studies

In the regeneration and reusability study of tepaPH beads, two different desorbing agents, 0.0001 M HCl and 0.0001 M HNO_3 were used. The same adsorption experimental conditions as stated previously were applied, and the used tepaPH beads were then subjected to the desorbing agents at room temperature for four hours. By applying the same experimental conditions, the adsorption-desorption process was repeated for five consecutive cycles.

RESULTS AND DISCUSSION

Characterization of the adsorbent

ATR-FTIR spectroscopy

Figure 1 shows the combined FTIR spectra of tepaPH beads before and after adsorption of MG, and the corresponding FTIR data are tabulated in Table 1. The functional groups were determined from the peaks present in the spectrum. By observing the spectrum before adsorption, the peak at 3410 cm^{-1} was broad and strong, which signified OH and NH stretching vibrations.[30-33] The peak observed at 2932 cm^{-1} can be attributed to the CH stretching vibration in methylene and methyl groups.[34-37] The presence of NH bending vibration in the amide bonds was indicated by the intense sharp peak at 1628 cm^{-1}.[33,36,37] The peak observed at 1511 cm^{-1} was due to the C=C stretching vibration of the aromatic ring, belonging to the lignin component in the peanut husks,[35,36,38-40] while the sharp medium peak at 1429 cm^{-1} represented the bending vibration of the hydroxyl group.[34] The absorption bands at 1372 cm^{-1} and 1268 cm^{-1} were caused by the vibration of CH_2 symmetric deformation and the C-N group, respectively. A broad peak observed near 1000 cm^{-1} was due to the overlapping peaks around 1032–1161 cm^{-1}, which indicates the overlapped stretching vibrations of C-O and C-N.[35-37] The stretching vibration of C-O-C observed at 893 cm^{-1} corresponds to the cellulose and hemicelluloses with β-1,4-glycosidic linkage.[41]

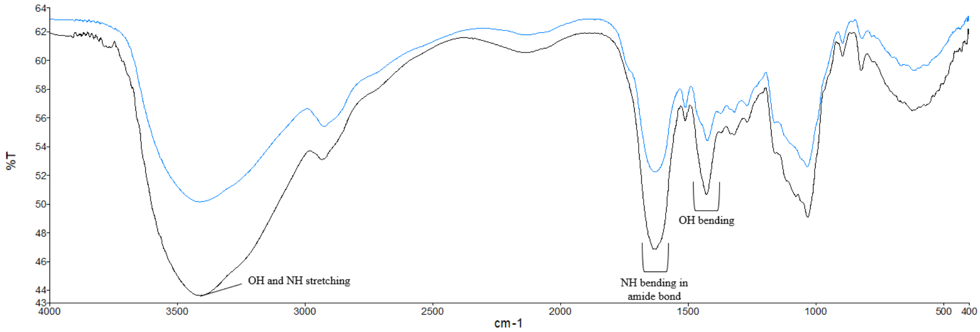

Figure 1: Infrared spectra of tepaPH beads before (black) and after (blue) adsorption of MG

Table 1
Assignment of IR absorption peaks for tepaPH beads before and after adsorption of MG

Functional group	Wavenumber (cm^{-1})	
	Before MG adsorption	After MG adsorption
OH and NH stretching	3410	3413
CH stretching	2932	2925
NH bending	1628	1627
C=C stretching	1511	1510
OH bending	1429	1424
C-O-C stretching	893	896

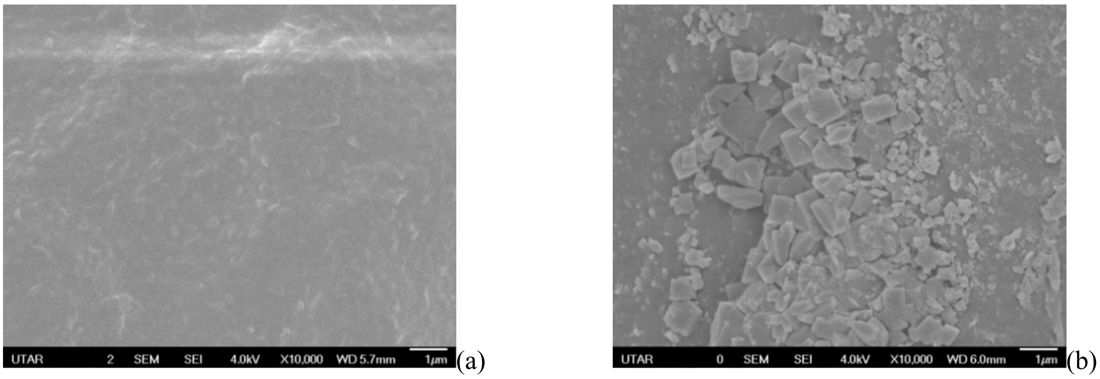

(a) (b)

Figure 2: 10000 × magnification SEM images of tepaPH beads: (a) unloaded with MG and (b) loaded with MG

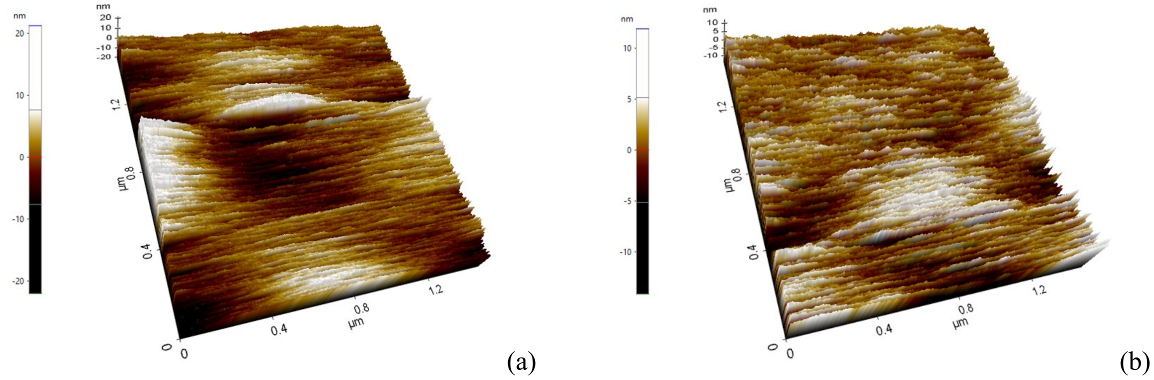

(a) (b)

Figure 3: AFM micrographs of tepaPH beads (a) unloaded with MG and (b) loaded with MG

After adsorption of MG, only a few absorption peaks in the FTIR spectrum of tepaPH beads show slight shifting in the wavenumber, as given in Table 1. However, the intensity of the peaks decreased after adsorption and this is most probably due to the interaction of tepaPH beads and MG, where chemical bonds were formed between the functional groups.[42,43] The intensity of the peaks at 3413 and 1424 cm^{-1}, representing the hydroxyl group, reduced significantly after MG adsorption. Loss of hydroxyl groups may be due to the reaction between the negatively charged hydroxyl group and the positively charged MG cation. Besides, the reduced intensity observed at 1627 cm^{-1} suggests the alteration of the amide group, as amide oxygen, which is negatively charged, attracts and binds with the MG cation.

The minimal differences observed are reasonable as dye adsorption is a surface chemistry process.[44] Furthermore, it can also be due to the instrument detection limit. This phenomenon was reported in previous studies using other agro-based materials for adsorption as well.[42,44–47]

SEM analysis

SEM was employed to study changes in surface morphology of the loaded and unloaded tepaPH beads with MG dye molecules. The SEM images presented in Figure 2 (a and b) were recorded before and after adsorption of MG by the adsorbent, respectively. The tepaPH beads' surface was non-porous and smooth. This observation agreed well with the findings reported by Mani *et al*.[35] and Chan *et al*.,[47] who noted that the surface of peanut husks is non-porous. After tepaPH beads were loaded with MG, a large number of cube-shaped particles were found agglomerated and adhered onto the composite beads surface, making it very rough and uneven. The presence of these cube-shaped particles has proven that MG was successfully adsorbed by tepaPH beads. Such interesting observations involving cube-shaped particles were also reported in previous works related to MG adsorption.[48]

AFM study

The possible changes that occurred in the surface structure of tepaPH beads on the atomic scale were studied using the atomic force microscopy technique. This technique uses the colour mapping method to denote low topography, with dark regions, and high topography, with light regions. As shown in Figure 3a, it is noticed that areas with darker colour were dominant before adsorption of MG. Those darker regions indicated a deep dent area on the adsorbent's surface. A powerful imaging tool, such as XEI software (version 4.3.4.Build22, Park System), can be useful in both qualitative and quantitative analysis involving surface roughness of the adsorbent.

The average roughness of tepaPH beads was 0.0029 µm and it reduced to 0.0020 µm with MG adsorbed onto its surface. Similarly, the root mean square roughness of tepaPH beads was 0.0039 µm and it reduced to 0.0026 µm after the composite beads surface was loaded with MG. The deep dent areas on the adsorbent surface were filled and coated with MG dye molecules, causing the reduction in surface roughness. Hence, light coloured areas were dominant after MG adsorption, as the adsorbent becomes more intense, which is significantly different from the findings for the adsorbent before the adsorption process.

Batch adsorption studies

Effect of contact time and initial MG concentration

The concentration of adsorbate and contact time play a critical role in the adsorption system. The adsorbent is considered as highly efficient when a rapid uptake of the pollutant is achieved in a short period of time. A similar adsorption trend was observed for all the three examined concentrations (10, 20, and 30 mg/L). The adsorption rate was high in the first 2 hours, and then it slowed down, eventually reaching equilibrium at 420 minutes. Song,[49] and Ahmad and Alrozi[26] have reported a similar adsorption trend for the uptake of MG by sawdust and rambutan peel-based activated carbon, respectively. At the beginning of the experiment, the surface of the adsorbent consists of a lot of unoccupied adsorption sites, hence, MG dye molecules can bind freely with any binding sites.[50] When the surface becomes more saturated, the adsorption rate gradually decreases as the number of vacant binding sites decreases. It is also more difficult to bind to the remaining binding sites because of the electrostatic repulsion between the adsorbed and free MG dye molecules.[26,46,51,52] As the adsorption process approaches equilibrium, the uptake of MG becomes very slow because of the reduced MG concentration and the uptake remained constant after equilibrium was attained. The adsorbent's surface is considered saturated with MG dye molecules.[53]

With lower initial MG concentration, a shorter contact time was required to attain the equilibrium, and *vice versa*. This is because at low MG concentration, the MG dye molecules have less competition for the binding sites and experience smaller repulsive force due to a low number of dye molecules. The adsorption capacity at 10 mg/L MG concentration was 0.76 mg/g and rose to 2.41 mg/g with 30 mg/L MG concentration. The adsorption capacity was greatly enhanced when there was a three-fold increase in dye concentration. The mass transfer resistance between the liquid and the solid phase can be overcome by the concentration gradient of the dye molecules.[26,49,54] High initial MG concentration provides a stronger mass transfer driving force and this improves the adsorbent and dye molecules' interaction.[21,49] Besides, when dye concentration increases, there is an increased number of dye molecules present in the solution for adsorption. Some previously studied works related to MG adsorption also reported similar results.[21,26,49,54,55]

Effect of pH

The ionization degree of a dye and the surface charge of an adsorbent are greatly influenced by the solution pH. So, the adsorption study of MG at various pH is necessary. The MG uptake at varying pH (2–9) was depicted in Figure 4. Malachite Green was not studied under extremely high or low pH (pH greater than 9 and pH below 2) because of its instability under these conditions. It was observed that MG turned yellow when the solution was strongly acidic and became colourless in strongly alkaline medium. However, the colour of MG is relatively stable in weakly acidic environment. This phenomenon has also been reported in a previous study.[49]

The MG adsorption was the highest from pH 4 to 6, as seen in Figure 4. Since the natural pH of MG is pH 4, no pH adjustment was carried out in subsequent experiments. The percentage uptake of MG was lowest at pH 2, where it was only 9.56%. This is because at low pH, the adsorbent surface undergoes protonation and becomes positively charged.[56] MG is a cationic dye with ions that are positively charged. Electrostatic repulsion between adsorbents and adsorbates will inhibit the attachment of MG onto tepaPH beads surface. Additionally, the excess hydrogen ions will compete for vacant binding sites with the dye molecules.[16,52,57] The percentage uptake of MG has a sharp increase to 81% at pH 4 and remained almost constant until pH 6. After that, the MG uptake gradually decreased to 64.15% at pH 9. Theoretically, cationic dye will have greater uptake under alkaline conditions, due to the deprotonated adsorbent surface, where electrostatic attraction is dominant. However, this was not observed in this study. The main reason for this is due to the instability of the MG dye solution under extreme pH conditions. As a result of this, the absorbance value (the control) showed a notable decrease and the color of the dye solution changes even in the absence of the adsorbent. This was probably the main reason that explained the low MG uptake, whereby the molecular structure of MG was altered at high solution pH.[49] Moreover, the formation of soluble hydroxyl complexes may also lead to reduced MG uptake at high pH solution.[16,52] A similar adsorption trend under the influence of pH in MG adsorption was also reported in previous literature.[16,49,52,53]

Effect of adsorbent dosage

As shown in Figure 5, the percentage uptake of MG increased with increasing dosage of tepaPH beads. The uptake of MG increased from 36.22% to 94.52%, when the adsorbent dosage was increased from 0.10 g to 0.60 g. A more favorable uptake was expected when the adsorbent dosage was increased due to the increase of active sites and total surface area.[16,21,47,58] Besides, there are also higher chances for the dye molecules to be attached to the free binding sites. However, it has also been demonstrated in some studies that, when too much of the adsorbent was added in, clustering aggregation and overlapping of active sites for binding can occur. This subsequently caused the adsorption capacity to decrease with increasing adsorbent dosage.[55,59] The optimum dosage was determined to be at 0.20 g and this value was selected in further tests to study the effects of other parameters.

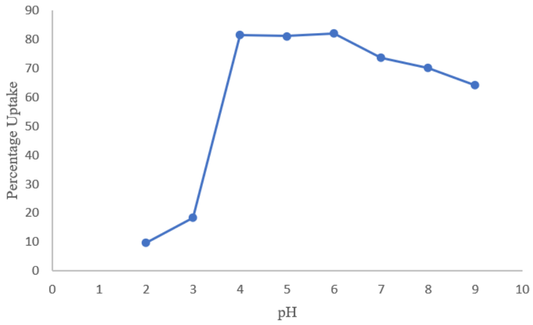

Figure 4: Effect of pH on percentage uptake of MG (conditions: 0.20 g tepaPH beads in 20 mL of 50 mg/L MG dye solution at 150 rpm for 7 h)

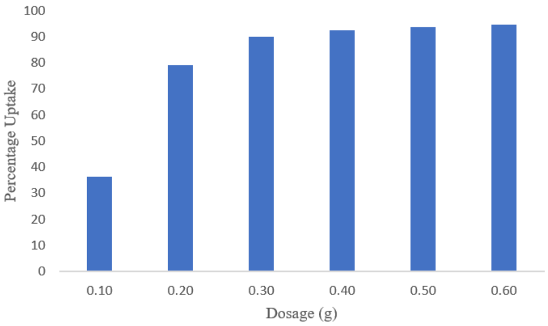

Figure 5: Effect of tepaPH beads dosage on percentage uptake of MG (conditions: 0.20 g tepaPH beads in 20 mL of 50 mg/L MG dye solution at 150 rpm for 7 h)

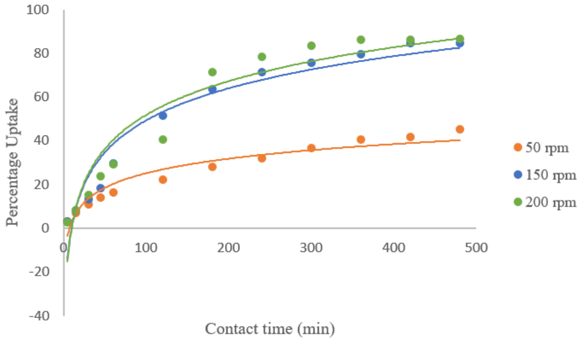

Figure 6: Effect of agitation rate as a function of contact time on percentage uptake of MG (conditions: 0.20 g of tepaPH beads in 20 mL of 50 mg/L MG dye solution for 7 h)

Effect of agitation rates

The MG adsorption trends obtained as a function of contact time, varying the agitation rates from 50 to 200 rpm, are shown in Figure 6. The MG uptake has a marked increase from 45.15% to 86.51%, when there was an increase in agitation rate from 50 to 200 rpm. The boundary layer thickness is diminished and the system will have higher turbulency when the agitation rate rises. With a higher agitation rate, the dye molecules will be having a higher diffusion rate from bulk liquid phase to the boundary film layer surrounding the adsorbent. As a result of this, an increase in the dye's uptake was observed.[60–62] The adsorption experiment performed at 200 rpm attained equilibrium in a shorter contact time, compared to agitation at 150 rpm, although the maximum percentage uptake values were very close. However, at the highest agitation rate, the detachment of the peanut husks from the composite beads was more prominent because of high collision of the beads. Khattri and Singh,[51] and Fil[55] have reported a similar trend for MG adsorption onto neem sawdust and montmorillonite clay, respectively.

Adsorption kinetic studies

The kinetics involved in the MG adsorption were analysed using two different equations, namely, the pseudo-1st-order (PFO) and pseudo-2nd-order (PSO) kinetic model equations. The linearised equation of the PFO model[63] is written as:

$$\log(q_e - q_t) = \log q_e - \frac{k_1}{2.303}t \qquad (1)$$

On the other hand, the PSO kinetic model linearized equation[64] is shown as:

$$\frac{t}{q_t} = \frac{1}{h} + \frac{t}{q_e} \qquad (2)$$

$$h = k_2 {q_e}^2 \qquad (3)$$

where q_e and q_t represent the amount of MG adsorbed at equilibrium and at time *t* (mg/g); k_1 and k_2 represent the rate constant of PFO kinetics (min^{-1}) and PSO kinetics (g/mg min) and h refers to the initial adsorption rate (mg/g min).

All the parameters of these two models were tabulated in Table 2. The coefficient of determination, R^2, of the PSO kinetic model had higher values and closer to unity compared to that of PFO. Therefore, it is apparent that the adsorption of MG onto tepaPH beads followed the PSO kinetic model. This model proposes the involvement of chemical sorption as the rate-limiting step.[64] The mechanism involves valency forces through electrons exchange or electrons sharing between the tepaPH beads and MG. As seen in Figure 7, the adsorption data are in a linear straight line, following PSO kinetic model throughout the experiment. Besides, Figure 8 shows that the experimental data agree well with the theoretically generated curves based on PSO. The calculated q_e agreed well with the experimental q_e. It was noticed that PSO kinetics rate constant k_2 decreased with increasing MG concentration. The affinity of MG dye molecules towards the adsorbent surface are lower when MG concentration is high because there is higher competition for the active sites, leading to reduced electrostatic interaction. Therefore, at high initial MG concentration, the adsorption rate is lower.

Table 2
Kinetic parameters at various MG concentrations

Initial MG concentration (mg/L)	PFO			PSO				Experimental
	q_e (mg/g)	k_1 (min^{-1})	R^2	q_e (mg/g)	h (mg/g·min)	k_2 (g/mg·min)	R^2	q_e (mg/g)
10	0.5284	9.6726×10^{-3}	0.9577	0.7385	0.02202	0.03425	0.9962	0.7394
20	1.4798	0.01495	0.9524	1.5452	0.02937	0.009232	0.9844	1.5361
30	3.4459	0.02119	0.9608	2.5064	0.03050	0.003218	0.9580	2.4050

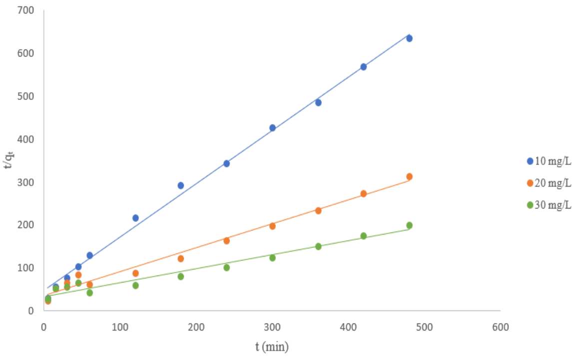

Figure 7: PSO kinetic model for adsorption of MG by tepaPH beads (0.20 g tepaPH beads in 20 mL of 10, 20 and 30 mg/L MG dye solution at 150 rpm for 7 h)

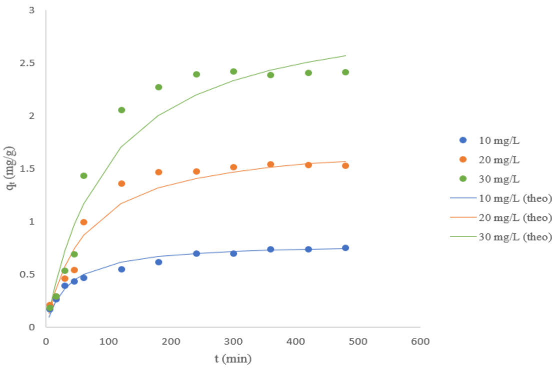

Figure 8: Theoretical (line) and experimental (symbol) data for PSO kinetics (0.20 g tepaPH beads in 20 mL of 10, 20 and 30 mg/L MG dye solution at 150 rpm for 7 h)

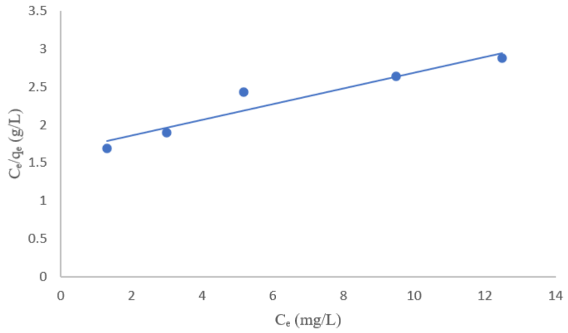

Figure 9: Langmuir isotherm for adsorption of MG (0.20 g of tepaPH beads in 20 mL of 10, 25, 30, 50 and 60 mg/L MG dye solution at 150 rpm for 7 h)

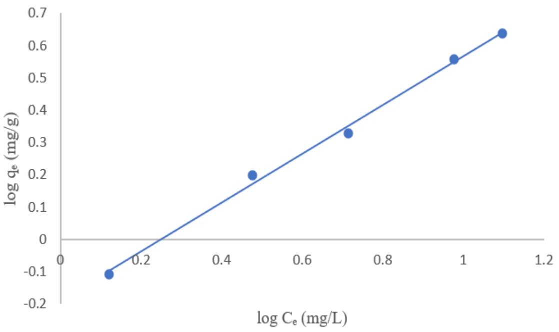

Figure 10: Freundlich isotherm for adsorption of MG (0.20 g of tepaPH beads in 20 mL of 10, 25, 30, 50 and 60 mg/L MG dye solution at 150 rpm for 7 h)

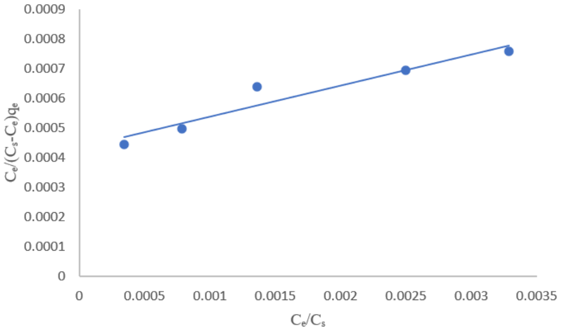

Figure 11: BET isotherm for adsorption of MG (conditions: 0.20 g of tepaPH beads in 20 mL of 10, 25, 30, 50 and 60 mg/L MG dye solution at 150 rpm for 7 h)

Adsorption isotherm studies

The Langmuir equation is defined as:

$$q_e = \frac{q_m K_L C_e}{1+K_L C_e} \tag{4}$$

The Langmuir isotherm model equation in linearized form is expressed as:

$$\frac{C_e}{q_e} = \frac{C_e}{q_m} + \frac{1}{K_L q_m} \tag{5}$$

where q_m = the maximum adsorption capacity (mg/g), K_L = the Langmuir constant related to energy of adsorbent (L/mg) and C_e = the concentration of adsorbate at equilibrium (mg/L). All other terms are as previously described. This isotherm model assumes the adsorbates adsorb onto adsorbent's active sites through chemical bonding and the adsorbates do not interact within themselves. The adsorption involves a monolayer coverage onto a homogeneous and comparable surface. Besides, only one adsorbate molecules can attach to each adsorption site.^{65}

The q_m and K_L values can be calculated from Figure 9 by using the gradient and y-intercept from the plot, and these values were determined to be 9.6339 mg/g and 0.0629 L/mg, respectively. The low R^2 value (0.9221) indicated the non-applicability of the Langmuir isotherm equation for the MG adsorption process. Table 3 presents the maximum adsorption capacity of different adsorbents used for MG adsorption.

The Freundlich isotherm is an exponential equation as shown:

$$q_e = K_F C_e^{\frac{1}{n}} \tag{6}$$

The Freundlich isotherm model linearized equation is illustrated as:

$$\log q_e = \frac{\log C_e}{n} + \log K_F \tag{7}$$

where n is the Freundlich constant for intensity, K_F is the Freundlich constant for adsorption capacity and all other terms are as previously described. This model assumes that the concentration of adsorbate rises with increasing adsorbate concentration on the surface of adsorbent. The adsorbent surface is heterogeneous and multiple layers of adsorbate molecules can be adsorbed onto the adsorbent surface through physicochemical sorption.^{70} The n value was calculated using the gradient from the linear plot in Figure 10, whereas the y-intercept was used to calculate the K_F value. The R^2 value of 0.9960 is very close to unity compared to the R^2 value obtained from Langmuir and BET isotherm models. This suggested that the Freundlich isotherm model provided reasonable fitting for the adsorption of MG. The interaction between MG dye molecules and tepaPH beads can be best explained by this model, where it assumes the adsorption is multilayer and the adsorbent surface is heterogeneous (Table 4).

The BET isotherm model is presented by the following equation:

$$q_e = \frac{K_B C_e q_m}{(C_s - C_e)\left[1 + (K_B - 1)\left(\frac{C_e}{C_s}\right)\right]} \tag{8}$$

The equation of BET isotherm model in linearized form is written as:

$$\frac{C_e}{(C_s - C_e) q_e} = \left(\frac{K_B - 1}{K_B q_m}\right)\left(\frac{C_e}{C_s}\right) + \frac{1}{K_B q_m} \tag{9}$$

where C_s is the saturation concentration of solute (mg/L) and K_B is the BET constant describing the energy of adsorbate-adsorbent interaction, whereas all other terms are as previously described. This isotherm model assumes homogeneous surface with multilayer adsorption, but the interaction between adsorbent and adsorbate is the strongest in the first layer. Also, the heat of adsorption for the first layer is different from those in the succeeding layers.[71] The y-intercept and gradient obtained from the graph in Figure 11 were substituted into Equation (9) to calculate the values of q_m and K_B. The K_B and q_m value were 262.5 and 9.5238 mg/g, respectively. The C_s value was determined as 3800 mg/L and the R^2 value was 0.9233. This low R^2 value indicates that the adsorption data is not fitted into this model.

Table 3

Comparison of the maximum adsorption capacities for MG by different adsorbents

Adsorbents	q_m (mg/g)	References
Cycas leave powder	39.0625	[6]
Wheat straw hydrochar	13.28	[16]
Tetraethylenepentamine modified peanut husks composite bead	9.6339	This work
chitosan 1-butyl-3-methylimidazolium acetate beads	8.07	[66]
Bentonite clay	7.716	[67]
Rice husks	6.5	[49]
SDS modified CPAC/chitosan composite	4.8	[68]
Coir pith activated carbon	4.4	[68]
Neem sawdust	4.354	[48]
Polylactide/spent brewery grains films	1.484	[69]
Chitosan 1-butyl-3-methylimidazolium beads	0.24	[66]

Table 4

Langmuir, Freundlich and BET isotherm parameters for MG adsorption

Langmuir		Freundlich		BET	
q_m (mg/g)	9.6339	n	1.3229	q_m (mg/g)	9.5238
K_L (L/mg)	0.0629	K_F	0.6477	K_B	262.5
R^2	0.9221	R^2	0.9960	R^2	0.9233

Experimental design studies

PB design

The PB design is an effective screening tool that can be used to identify the significant factors that can have a major impact on a system from a great number of factors, by performing a minimum run of experiments.[72] The agitation rate, adsorbent dosage, initial MG concentration and contact time were the factors studied in PB regarding their effects on the removal of MG by tepaPH beads. The effect of pH was excluded because of the instability of MG dye solution at pH below 2 and greater than pH 9. Besides, based on the results from the batch study, it has also been shown that the optimum removal of MG occurred at the natural pH of the dye solution. Table 5 provides the ANOVA data generated by Design Expert Software Version 7.1.3. A total of 12 experimental runs with the generated experimental conditions are shown in Table 6. The predicted and experimental percentage removal of MG was tabulated in the same table.

In this work, the effect of dosage, initial MG concentration and contact time were the three significant factors chosen as their p-values were lower than 0.05. The agitation rate was eliminated from the RSM because of having the p-value of 0.5972, which signified it has an insignificant influence on this adsorption system.

Validation of PB design model

In order to verify the validity of the PB design model, the function of desirability was used. The experimental runs with the optimum desirability were performed. The percentage difference for each set of experimental runs ranged from 0.50 to12.66%. These deviations might be due to the involvement of the insignificant factor.

Table 5
ANOVA of PB for MG adsorption by tepaPH beads

Source	Sum of squares	df	Mean square	F value	p-value
Model	7723.76	4	1930.94	27.88	0.0002
A-Contact time	3957.22	1	3957.22	57.15	0.0001
B-Initial MG concentration	485.42	1	485.42	7.01	0.0331
C-Dosage	3259.91	1	3259.91	47.08	0.0002
D-Agitation rate	21.21	1	21.21	0.31	0.5972
Residual	484.73	7	69.25		

Table 6
PB design and results for MG adsorption by tepaPH beads

Experimental run	Factor				Experimental % uptake	Predicted % uptake
	Contact time (min)	Initial MG concentration (mg/L)	Dosage (g)	Agitation rate (rpm)		
1	5	50	0.6	50	31.39	36.05
2	5	50	0.1	200	4.04	5.74
3	5	10	0.6	50	52.20	48.77
4	5	10	0.1	200	20.90	18.46
5	5	50	0.6	200	36.22	38.71
6	5	10	0.1	50	18.78	15.80
7	480	50	0.1	200	51.83	42.06
8	480	10	0.6	200	84.45	83.51
9	480	10	0.1	50	51.29	52.12
10	480	50	0.1	50	26.75	39.40
11	480	50	0.6	50	84.10	72.37
12	480	10	0.6	200	83.02	83.51

Optimization study: RSM

For the optimization study, three factors, including tepaPH beads dosage, initial MG concentration and contact time, were selected to determine their combined effects to achieve the maximum MG uptake. The software has generated 15 sets of experimental runs and a modified cubic model equation. The following modified cubic model equation can be used to predict the percentage uptake of MG with coded terms, where A is the contact time, B is the initial MG concentration, and C is the dosage:

$$\text{Percentage uptake} = -1.42868 + 0.27582 * A + 0.12174 * B + 184.35547 * C + 1.07914\times10^{-3} * AB + 0.020826 * AC + 0.31206 * BC - 4.25735\times10^{-4} * A^2 - 0.010937 * B^2 - 194.35317 * C^2 \qquad (10)$$

Table 7 shows the ANOVA data generated by RSM based on the results obtained from the designed experiments. It can be deduced that this model is significant as the p-value was smaller than 0.05. The value of R^2 will increase when new terms are added into the model, while the value of adjusted R^2 will decrease with the addition of non-significant terms. For this reason, the R^2 and adjusted R^2 values must not have a large difference with one another.[73] The R^2 and adjusted R^2 were found to be 0.9820 and 0.9657, respectively, thus being very close to each other. High R^2 value implied that the predicted response agreed well with experimental results, while the significance of the factors was further confirmed by the high adjusted R^2 value.[74] Besides, the predicted R^2 also agreed reasonably with the adjusted R^2. An adequate precision, 25.226, was obtained (a value greater than 4), implying an adequate signal for this adsorption process.

From RSM, the 3D surface plots were generated to show the correlation between three significant factors and their response. The 3D surface plot that illustrates the effect of initial MG concentrations and contact time towards the MG uptake is shown in Figure 12. The maximum MG uptake was attained when the initial MG concentration is low and for a prolonged period of time. By increasing the contact time, this allows a better interaction between MG dye molecules and tepaPH beads, and therefore, the uptake of MG increased. Comparing with the other two factors, the influence of initial MG concentration on this system was weaker. This may be due to the relatively higher p-value.[47] With low initial MG concentrations, better MG uptake was achieved, because there was a lower number of dye molecules to bind to the adsorbent's surface. In other words, the dye molecules have sufficient binding sites to accommodate them. When the number of MG dye molecules rises with increasing initial MG concentration, the adsorption sites are easily saturated with dye molecules, and this causes low MG uptake.

The correlation between the effect of dosage, contact time and the MG uptake is represented in Figure 13. It can be observed that with increasing tepaPH beads dosage, the percentage uptake of MG increased. There is a higher capacity for the adsorbent to accommodate MG dye molecules due to a greater number of binding sites and a higher total surface area. The competition between MG dye molecules for unoccupied binding sites was greatly diminished. A similar adsorption pattern to that in Figure 12 was observed in this plot, where the MG uptake increased with contact time. The optimum condition for MG uptake was achieved at high adsorbent dosage and long contact time.

Table 7
ANOVA of RSM for MG adsorption by tepaPH beads

Source	Sum of squares	df	Mean square	F value	p-value
Model	15925.99	9	1769.55	60.45	< 0.0001
A-Contact time	6702.20	1	6702.20	228.96	< 0.0001
B-Initial MG concentration	107.01	1	107.01	3.66	0.0849
C-Dosage	2458.65	1	2458.65	83.99	< 0.0001
AB	210.20	1	210.20	7.18	0.0231
AC	12.23	1	12.23	0.42	0.5326
BC	19.48	1	19.48	0.67	0.4337
A^2	1585.86	1	1585.86	54.18	< 0.0001
B^2	52.63	1	52.63	1.80	0.2096
C^2	405.77	1	405.77	13.86	0.0040
Residual	292.73	10	29.27		
Lack of Fit	292.73	5	58.55		

Note: R^2: 0.9820, adjusted R^2: 0.9657, predicted R^2: 0.7846, adequate precision: 25.226 and C.V.: 8.01%

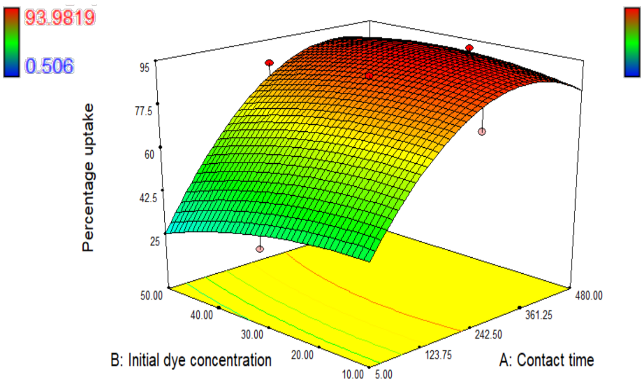

Figure 12: RSM 3D surface plot for the % uptake of MG by tepaPH beads (A - contact time and B - initial MG concentrations)

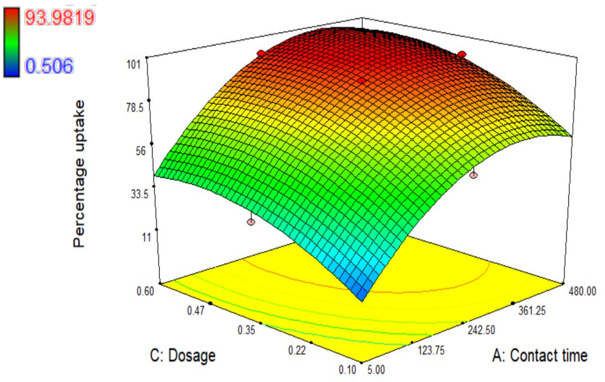

Figure 13: RSM 3D surface plot for the % uptake of MG by tepaPH beads (A - contact time and C - tepaPH beads dosage)

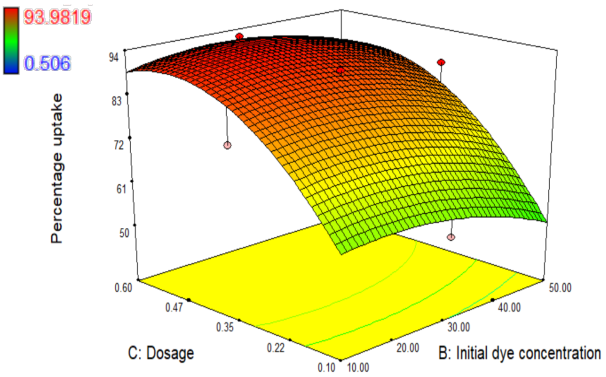

Figure 14: RSM 3D surface plot for the % uptake of MG by tepaPH beads (B - Initial MG concentrations and C - tepaPH beads dosage)

Table 8
RSM design and results for MG uptake (%) by tepaPH beads

Experimental run	Factor			Experimental % uptake	Predicted % uptake
	Contact time	Initial MG conc.	Dosage		
1	5	10	0.1	17.43	16.93
2	5	50	0.1	0.51	- 2.98
3	5	10	0.6	48.50	42.70
4	5	50	0.6	24.72	29.02
5	5	30	0.35	32.46	37.94
6	242.5	10	0.35	77.73	86.74
7	242.5	50	0.35	85.41	80.20
8	242.5	30	0.1	55.63	60.02
9	242.5	30	0.6	91.96	91.38
10	242.5	30	0.35	89.11	87.84
11	480	10	0.1	61.24	55.98
12	480	50	0.1	51.72	56.57
13	480	10	0.6	84.16	86.70
14	480	50	0.6	93.98	93.53
15	480	30	0.35	91.40	89.72

The correlation between tepaPH beads dosage, initial MG concentration and MG uptake is illustrated in Figure 14. By using high adsorbent dosage and low MG concentration, this situation is beneficial towards the MG uptake. A similar adsorption pattern for initial MG concentration is presented in Figure 12. By increasing the adsorbent dosage, this corresponds to an increase in active sites for the adsorption and subsequently enhancing the MG removal.

Verification of RSM

The function of desirability was used to validate this model to ensure that this model is reliable and generates results with high accuracy. The experimental runs with the highest desirability were performed. The percentage difference for each set of experimental runs ranged between 0.45–9.01%. The predicted and experimental results of MG uptake were tabulated in Table 8, along with the experimental conditions for each run.

Regeneration and reusability studies

In order to examine the capability and effectiveness of an adsorbent to be applied in practical application, it is crucial to evaluate the reusability of the adsorbent. Figure 15 shows the percentage uptake of MG after desorption using two different desorbing agents. From the results, the MG dye uptake decreased with the number of reuse cycles for both desorbing agents. Still, as demonstrated in this adsorption-desorption trend, clearly, HNO_3 is a better desorbing agent, as compared to HCl. Although after each cycle, the MG removal efficiency is decreasing gradually, an uptake greater than 50% is still obtainable after five cycles. This clearly implies that tepaPH beads can be reused for adsorption of MG.

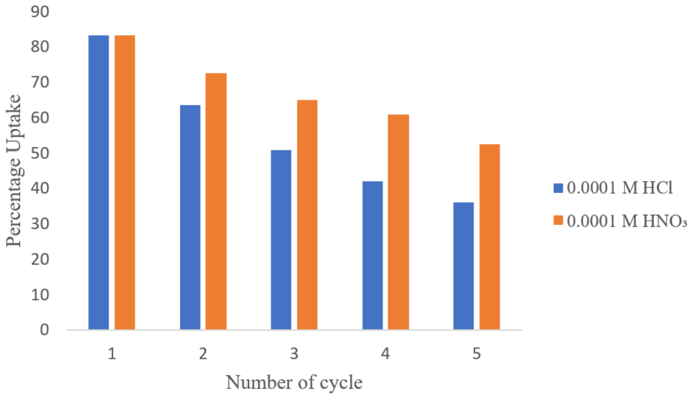

Figure 15: Effect of desorbing agents on percentage uptake of MG (conditions: tepaPH beads in 20 mL of 20 mg/L MG dye solution at 150 rpm for 4 h)

Dahri and co-workers have reported a similar adsorption trend obtained when using HNO_3 as a desorbing agent for MG in order to regenerate a walnut shell adsorbent.[75] Similar results were also reported by El Messaoudi *et al.*, who reported that the adsorption of Congo Red by *Zizyphus lotus* jujube shells reduced by 30.6% after four reuse cycles.[76] Furthermore, the Congo Red adsorption by alginate/natural bentonite composite beads also decreased with each cycle, and the adsorption efficiency dropped by nearly 40% after the fifth regeneration cycle.[77]

CONCLUSION

The effectiveness of tepaPH beads in the removal of MG has been demonstrated in batch studies. The overall higher R^2 values denoted that the adsorption system followed the PSO kinetic model rather than the PFO kinetic model. This adsorption process also obeyed the Freundlich isotherm model, which suggests that the adsorbent surface is heterogeneous and the adsorption is multilayer. By employing the PB design, the parameters that significantly affect the MG uptake were found to be tepaPH beads dosage, initial MG concentration and contact time. The percentage uptake of MG and the correlation between significant factors were illustrated in the RSM 3D surface plots. With 0.6 g of adsorbent dosage, 50 mg/L of initial MG concentration, and 480 minutes of contact time, the maximum MG uptake can achieve 93.98%.

ACKNOWLEDGEMENTS: This research work received the financial support and research facilities assistance from Universiti Tunku Abdul Rahman.

REFERENCES

[1] S. L. Lee, S. W. Liew and S. T. Ong, *Acta Chim. Slov.*, **63**, 144 (2016), https://doi.org/10.17344/acsi.2015.2068

[2] L. Bulgariu, L. B. Escudero, O. S. Bello, M. Iqbal, J. Nisar *et al.*, *J. Mol. Liq.*, **276**, 728 (2019), https://doi.org/10.1016/j.molliq.2018.12.001

[3] M. F. Mohamad Yusop, A. Z. Abdullah and M. A. Ahmad, *Diam. Relat. Mater.*, **136**, 10991 (2023), https://doi.org/10.1016/j.diamond.2023.109991

[4] P. Senthil Kumar, G. Janet Joshiba, C. C. Femina, P. Varshini, S. Priyadharshini *et al.*, *Desalin. Water Treat.*, **172**, 395 (2019), https://doi.org/10.5004/dwt.2019.24613

[5] M. Raninga, A. Mudgal, V. K. Patel, J. Patel and M. K. Sinha, *Mater. Today Proc.*, **77**, 286 (2023), https://doi.org/10.1016/j.matpr.2022.11.358

[6] S. D. Salman, Z. R. Zair and Z. T. Alismaeel, *Desalin. Water Treat.*, **317**, 100246 (2024), https://doi.org/10.1016/j.dwt.2024.100246.

[7] R. Jain, P. Sharma, S. Sikarwar, J. Mittal and D. Pathak, *Desalin. Water Treat.*, **52**, 7776 (2014), https://doi.org/10.1080/19443994.2013.837009

[8] J. Mittal, R. Ahmad, A. Mariyam, V. K. Gupta and A. Mittal, *Desalin. Water Treat.*, **210**, 365 (2021), https://doi.org/10.5004/dwt.2021.26562

[9] A. Mariyam, J. Mittal, F. Sakina, R. T. Baker, A. K. Sharma *et al.*, *Arab. J. Chem.*, **14**, 103186 (2021), https://doi.org/10.1016/j.arabjc.2021.103186

[10] A. Patel, S. Soni, J. Mittal, A. Mittal and C. Arora, *Desalin. Water Treat.*, **220**, 342 (2021), https://doi.org/10.5004/dwt.2021.26911

[11] F. Chouli, A. O. Ezzat, L. Sabantina, A. Benyoucef and A. Zehhaf, *Molecules*, **29**, 54 (2024), https://doi.org/10.3390/molecules29010054

[12] A. Saravanan, P. S. Kumar, D. V. N. Vo, S. Swetha, P. T. Ngueagni *et al.*, *Chemosphere*, **271**, 129484 (2021), https://doi.org/10.1016/j.chemosphere.2020.129484

[13] A. Saravanan, P. S. Kumar, R. V. Hemavathy, S. Jeevanantham, P. Harikumar *et al.*, *Sci. Total Environ.*,

812, 152456 (2022), https://doi.org/10.1016/j.scitotenv.2021.152456

[14] C. Arora, P. Kumar, S. Soni, J. Mittal, A. Mittal *et al.*, *Desalin. Water Treat.*, **195**, 341 (2020), https://doi.org/10.5004/dwt.2020.25897

[15] C. Arora, D. Sahu, D. Bharti, V. Tamrakar, S. Soni *et al.*, *Desalin. Water Treat.*, **167**, 324 (2019), https://doi.org/10.5004/dwt.2019.24595

[16] S. Kohzadi, N. Marzban, Y. Zandsalimi, K. Godini, N. Amini *et al.*, *Heliyon*, **9**, e21258 (2023), https://doi.org/10.1016/j.heliyon.2023.e21258

[17] E. Kavci, *Chem. Eng. Commun.*, **208**, 318 (2020), https://doi.org/10.1080/00986445.2020.1715961

[18] F. Mashkoor and A. Nasar, *J. Mol. Liq.*, **274**, 315 (2019), https://doi.org/10.1016/j.molliq.2018.10.119

[19] L. Zhao, W. Lv, J. Hou, Y. Li, J. Duan *et al.*, *Microchem. J.*, **152**, 104425 (2020), https://doi.org/10.1016/j.microc.2019.104425

[20] Z. Shi, C. Xu, F. Chen, Y. Wang, L. Li *et al.*, *RSC Adv.*, **7**, 49947 (2017), https://doi.org/10.1039/c7ra10912a

[21] J. S. Algethami, M. A. M. Alhamami, A. A. Alqadami, S. Melhi and A. F. Seliem, *Int. J. Biol. Macromol.*, **254**, 127767 (2024), https://doi.org/10.1016/j.ijbiomac.2023.127767

[22] M. S. Bashanaini, M. H. Al-Douh and H. S. Al-Ameri, *Sci. J. Anal. Chem.*, **7**, 42 (2019), https://doi.org/10.11648/j.sjac.20190702.12

[23] M. Jiang, L. Chen and N. Niu, *J. Mol. Struct.*, **1260**, 132842 (2022), https://doi.org/10.1016/j.molstruc.2022.132842

[24] J. Wu, J. Yang, P. Feng, L. Wen, G. Huang *et al.*, *J. Ind. Eng. Chem.*, **113**, 206 (2022), https://doi.org/10.1016/j.jiec.2022.05.047

[25] O. Baytar, A. A. Ceyhan and Ö. Şahin, *Int. J. Phytoremed.*, **23**, 693 (2020), https://doi.org/10.1080/15226514.2020.1849015

[26] M. A. Ahmad and R. Alrozi, *Chem. Eng. J.*, **171**, 510 (2011), https://doi.org/10.1016/j.cej.2011.04.018.

[27] United States Department of Agricultural, World Agricultural Production, 2024, https://fas.usda.gov/data/world-agricultural-production-03082024 (accessed June 25, 2024)

[28] Inamuddin, A. Mohammad and A. M. Asiri, “Inorganic Pollutants in Wastewater: Methods Of Analysis, Removal and Treatment”, Materials Research Forum LLC, Millersville, USA, 2017, https://books.google.com.my/books?id=tJVLDwAAQBAJ

[29] H. M. El Refay, A. Goma, N. Badawy and F. Al Zahra Ghanem, *Egypt. J. Chem.*, **65**, 97 (2022), https://doi.org/10.21608/ejchem.2022.102614.4757

[30] X. Y. Huang, X. Y. Mao, H. T. Bu, X. Y. Yu, G. B. Jiang *et al.*, *Carbohyd. Res.*, **346**, 1232 (2011), https://doi.org/10.1016/j.carres.2011.04.012

[31] G. B. Jiang, Z. T. Lin, X. Y. Huang, Y. Q. Zheng, C. C. Ren *et al.*, *Int. J. Biol. Macromol.*, **50**, 707 (2012), https://doi.org/10.1016/j.ijbiomac.2011.12.030

[32] A. M. Omer, R. E. Khalifa, Z. Hu, H. Zhang, C. Liu *et al.*, *Int. J. Biol. Macromol.*, **125**, 1221 (2019), https://doi.org/10.1016/j.ijbiomac.2018.09.097

[33] X. Tang, P. Tang and L. Liu, *J. Braz. Chem. Soc.*, **29**, 334 (2018), https://doi.org/10.21577/0103-5053.20170145

[34] S. Sunkar, P. Prakash, B. Dhandapani, O. Baigenzhenov, J. A. Kumar *et al.*, *Environ. Res.*, **233**, 116486 (2023), https://doi.org/10.1016/j.envres.2023.116486

[35] D. Mani, D. Elango, A. Priyadharsan, L. A. Al-Humaid, N. D. Al-Dahmash *et al.*, *Environ. Res.*, **231**, 116026 (2023), https://doi.org/10.1016/j.envres.2023.116026

[36] P. Ghosh, S. Saha, R. Kumar Bishwas, S. Karmaker and T. K. Saha, *Cellulose Chem. Technol.*, **56**, 443 (2022), https://doi.org/10.35812/CelluloseChemTechnol.2022.56.38

[37] M. Ghasemi, S. Mashhadi, M. Asif, I. Tyagi, S. Agarwal *et al.*, *J. Mol. Liq.*, **213**, 317 (2016), https://doi.org/10.1016/j.molliq.2015.09.048

[38] J. Song, W. Zou, Y. Bian, F. Su and R. Han, *Desalination*, **265**, 119 (2011), https://doi.org/10.1016/j.desal.2010.07.041

[39] S. Zhang, R. Zhang, W. Xiao and R. Han, *Water Sci. Technol.*, **68**, 2158 (2013), https://doi.org/10.2166/wst.2013.464

[40] M. Picard, S. Thakur, M. Misra, D. F. Mielewski and A. K. Mohan, *Sci. Rep.*, **10**, 3310 (2020), https://doi.org/10.1038/s41598-020-59582-3

[41] J. Zhuang, M. Li, Y. Pu, A. J. Ragauskas and C. G. Yoo, *Appl. Sci.*, **10**, 4345 (2020), https://doi.org/10.3390/app10124345

[42] A. S. Sartape, A. M. Mandhare, V. V. Jadhav, P. D. Raut, M. A. Anuse *et al.*, *Arab. J. Chem.*, **10**, S3229 (2017), https://doi.org/10.1016/j.arabjc.2013.12.019

[43] F. Bouaziz, M. Koubaa, F. Kallel, R. E. Ghorbel and S. E. Chaabouni, *Int. J. Biol. Macromol.*, **105**, 56 (2017), https://doi.org/10.1016/j.ijbiomac.2017.06.106

[44] C. I. Tay and S. T. Ong, *J. Phys. Sci.*, **30**, 137 (2019), https://doi.org/10.21315/jps2019.30.2.8

[45] H. Y. Gan, L. E. Leow and S. T. Ong, *Acta Chim. Slov.*, **64**, 144 (2017), https://doi.org/10.17344/acsi.2016.2983

[46] L. Das, P. Das, A. Bhowal and C. Bhattachariee, *J. Environ. Manage.*, **276**, 111272 (2020), https://doi.org/10.1016/j.jenvman.2020.111272

[47] K. T. Chan, S. T. Ong and S. T. Ha, *Desalin. Water Treat.*, **317**, 100060 (2024), https://doi.org/10.1016/j.dwt.2024.100060

[48] X. Fan, L. Deng, K. Li, H. Lu, R. Wang *et al.*, *Colloid. Interface Sci. Commun.*, **44**, 100485 (2021), https://doi.org/10.1016/j.colcom.2021.100485

[49] Y. Song, S. Ding, S. Chen, H. Xu, Y. Mei *et al.*, *Korean J. Chem. Eng.*, **32**, 2443 (2015), https://doi.org/10.1007/s11814-015-0103-1

[50] M. Wang, Y. Jiao, N. Li and Y. Su, *J. Alloys Compd.*, **969**, 172344 (2023), https://doi.org/10.1016/j.jallcom.2023.172344

[51] S. D. Khattri and M. K. Singh, *J. Hazard. Mater.*, **167**, 1089 (2009), https://doi.org/10.1016/j.jhazmat.2009.01.101

[52] V. M. Muinde, J. M. Onyari, B. Wamalwa, J. Wabomba and R. M. Nthumbi, *J. Environ. Prot.*, **8**, 215 (2017), https://doi.org/10.4236/jep.2017.83017

[53] S. Arellano-Cárdenas, S. López-Cortez, M. Cornejo-Mazón and J. C. Mares-Gutiérrez, *Appl. Surf. Sci.*, **280**, 74 (2013), https://doi.org/10.1016/j.apsusc.2013.04.097

[54] M. A. Ahmad, N. Ahmad and O. S. Bello, *Water Air Soil Pollut.*, **225**, 2057 (2014), https://doi.org/10.1007/s11270-014-2057-z

[55] B. A. Fil, *Particulate Sci. Technol.*, **34**, 118 (2016), https://doi.org/10.1080/02726351.2015.1052122

[56] E. Makhado, B. R. Motshabi, D. Allouss, K. E. Ramohlola, K. D. Modibane *et al.*, *Chemosphere*, **306**, 135524 (2022), https://doi.org/10.1016/j.chemosphere.2022.135524

[57] B. H. Hameed and M. I. El-Khaiary, *J. Hazard. Mater.*, **153**, 701 (2008), https://doi.org/10.1016/j.jhazmat.2007.09.019

[58] A. Hojjati-Najafabadi, P. Nasr Esfahani, F. Davar, T. M. Aminabhavi and Y. Vasseghian, *Chem. Eng. J.*, **471**, 144485 (2023), https://doi.org/10.1016/j.cej.2023.144485

[59] J. Zhang, Y. Li, C. Zhang and Y. Jing, *J. Hazard. Mater.*, **150**, 774 (2008), https://doi.org/10.1016/j.jhazmat.2007.05.036

[60] S. Ghorai, A. K. Sarkar, A. B. Panda and S. Pal, *Bioresour. Technol.*, **144**, 485 (2013), https://doi.org/10.1016/j.biortech.2013.06.108

[61] G. K. Latinwo, A. O. Alade, S. E. Agarry and E. O. Dada, *Polycycl. Aromat. Compd.*, **41**, 400 (2019), https://doi.org/10.1080/10406638.2019.1591467

[62] H. Q. Ali and A. A. Mohammed, *Iraqi J. Chem. Petrol. Eng.*, **21**, 21 (2020), https://doi.org/10.31699/ijcpe.2020.4.3

[63] S. K. Lagergren, *Sven. Vetenskapsakad. Handingarl*, **24**, 1 (1898)

[64] Y.S. Ho and G. Mckay, *Process Biochem.*, **34**, 451 (1999)

[65] I. Langmuir, *J. Am. Chem. Soc.*, **40**, 1361 (1918)

[66] F. Naseeruteen, N. S. A. Hamid, F. B. M. Suah, W. S. W. Ngah and F. S. Mehamod, *Int. J. Biol. Macromol.*, **107**, 1270 (2018), https://doi.org/10.1016/j.ijbiomac.2017.09.111

[67] S. S. Tahir and N. Rauf, *Chemosphere*, **63**, 1842 (2006), https://doi.org/10.1016/j.chemosphere.2005.10.033

[68] T. K. Arumugam, P. Krishnamoorthy, N. R. Rajagopalan, S. Nanthini and D. Vasudevan, *Int. J. Biol. Macromol.*, **128**, 655 (2019), https://doi.org/10.1016/j.ijbiomac.2019.01.185

[69] H. A. Chanzu, J. M. Onyari and P. M. Shiundu, *J. Polym. Environ.*, **20**, 665 (2012), https://doi.org/10.1007/s10924-012-0479-5

[70] H. Freundlich, *J. Phys. Chem.*, **57**, 385 (1906)

[71] S. Brunauer, P. H. Emmett and E. Teller, *J. Am. Chem. Soc.*, **60**, 309 (1938)

[72] R. Thiruchelvi, R. Venkataraghavan and D. Sharmila, *Mater. Today Proc.*, **37**, 1859 (2021), https://doi.org/10.1016/j.matpr.2020.07.448

[73] R. H. Myers and D. C. Montgomery, "Response Surface Methodology: Process and Product Optimization Using Designed Experiments", John Wiley & Sons Inc, 1995

[74] E. A. Dil, M. Ghaedi, A. Asfaram, S. Hajati, F. Mehrabi and A. Goudarzi, *Ultrason. Sonochem.*, **34**, 677 (2017), https://doi.org/10.1016/j.ultsonch.2016.07.001

[75] M. K. Dahri, M. R. R. Kooh and L. B. L. Lim, *J. Environ. Chem. Eng.*, **2**, 1434 (2014), https://doi.org/10.1016/j.jece.2014.07.008

[76] N. El Messaoudi, M. El. Khomri, N. Chlif, Z. G. Chegini, A. Dbik *et al.*, *Groundw. Sustain. Dev.*, **12**, 100552 (2021), https://doi.org/10.1016/j.gsd.2021.100552

[77] A. Oussalah, A. Boukerroui, A. Aichour and B. Djellouli, *Int. J. Biol. Macromol.*, **124**, 854 (2019), https://doi.org/10.1016/j.ijbiomac.2018.11.197